Kinematics and hydrodynamics of linear acceleration in eels, *Anguilla rostrata*

Eric D. Tytell

Department of Organismic and Evolutionary Biology, Harvard University, 26 Oxford Street, Cambridge, MA 02138, USA
(*tytell@oeb.harvard.edu*)

The kinematics and hydrodynamics of routine linear accelerations were studied in American eels, *Anguilla rostrata*, using high-speed video and particle image velocimetry. Eels were examined both during steady swimming at speeds from 0.6 to 1.9 body lengths (L) per second and during accelerations from -1.4 to $1.3\,L\,s^{-2}$. Multiple regression of the acceleration and steady swimming speed on the body kinematics suggests that eels primarily change their tail-tip velocity during acceleration. By contrast, the best predictor of steady swimming speed is body wave speed, keeping tail-tip velocity an approximately constant fraction of the swimming velocity. Thus, during steady swimming, Strouhal number does not vary with speed, remaining close to 0.32, but during acceleration, it deviates from the steady value. The kinematic changes during acceleration are indicated hydrodynamically by axial fluid momentum in the wake. During steady swimming, the wake consists of lateral jets of fluid and has minimal net axial momentum, which reflects a balance between thrust and drag. During acceleration, those jets rotate to point downstream, adding axial momentum to the fluid. The amount of added momentum correlates with the acceleration, but is greater than the necessary inertial force by 2.8 ± 0.6 times, indicating a substantial acceleration reaction.

Keywords: acceleration; anguilliform fish swimming; eels; manoeuvring; fluid dynamics; *Anguilla rostrata*

1. INTRODUCTION

Most studies of fish swimming have focused on extreme behaviours at two ends of a spectrum. At one end of the spectrum are many studies examining steady swimming, both from kinematic (Jayne & Lauder 1995; Donley & Dickson 2000) and hydrodynamic viewpoints (Müller *et al.* 1997, 2001; Drucker & Lauder 2001; Nauen & Lauder 2002; Tytell & Lauder 2004). At the other end of the spectrum are studies of very rapid behaviours such as fast starts and feeding strikes, primarily focusing on kinematics (Domenici & Blake 1997). However, anyone who has watched fishes swimming in nature will realize that most fishes rarely swim steadily or perform fast starts. Most of their time is filled with low-speed turns and small accelerations (Webb 1991).

Manoeuvres such as turning, however, are complicated and difficult to quantify, as is evidenced by the number of parameters collected about fast starts (Domenici & Blake 1997). However, linear acceleration, a simple yet important manoeuvre, has received no attention, and is probably quite important in normal fish swimming. Fishes accelerate linearly any time they change speed, and particularly when they hold position in a variable speed or turbulent flow.

To understand linear acceleration, it is important to separate acceleration effects from those resulting from steady motion. The eel, *Anguilla* spp., an anguilliform swimmer, has an unusual wake that makes this separation straightforward. In contrast to carangiform swimmers, which produce wakes with substantial rearward (axial) flow during steady swimming (Müller *et al.* 1997; Drucker & Lauder 2001; Nauen & Lauder 2002), eels' wakes have little axial flow (Müller *et al.* 2001; Tytell 2004). Tytell (2004) found that an eel's wake during steady swimming consists primarily of fluid jets pointed at $90°$ to the swimming direction, resulting in negligible fluid momentum in the axial direction.

The lack of axial momentum indicates zero net force, which should be expected based on Newton's laws because the eels were swimming at constant velocity (Tytell & Lauder 2004). In other words, during steady swimming, a fish's momentum does not change, so the momentum of the fluid around it must not change. By contrast, during an acceleration the fish's momentum does change, so the wake momentum must also change. Because of the small axial wake momentum during steady swimming, this change should be immediately apparent in an eel's wake.

This study provides, to the author's knowledge, the first quantitative description of how swimming kinematics and hydrodynamics change as eels perform routine linear accelerations. The kinematic parameters that change most during acceleration are identified and are compared with acceleration magnitude. Changes in wake momentum are identified to estimate the forces involved. The kinematic and hydrodynamic data together indicate a mechanism that eels use to perform small linear accelerations and change their swimming velocity.

2. MATERIAL AND METHODS
(a) *Experimental procedure*

American eels (*Anguilla rostrata*) were collected by seine from the Charles River (Cambridge, MA, USA) during June and July 2002 and housed in aquaria at room temperature. Experiments were conducted in a 600 l closed-circuit flow tank with a 26 cm wide × 26 cm deep × 80 cm long working section. Animals were confined to the working section using plastic grids covered in a fine mesh.

Before the experimental procedure, an eel was allowed to acclimate in the flow tank at a slow swimming velocity for at least 1 h. After the acclimation period, eels adopted a steady swimming behaviour. During the procedure, the animal was gently man-oeuvred into position by using a wooden probe. After a period of steady swimming, all eels accelerated voluntarily out of the filming region. Swimming was filmed from below through a front-surface mirror at 45° using a digital high-speed camera (RedLake) at 125 or 250 frames per second (fps).

To quantify flow velocities behind the swimming eel, the tank was seeded with near-neutrally buoyant silver-coated glass parti-cles (12 μm in diameter; density $1.3\,\text{g cm}^{-3}$; Potters Industries, USA). As the particles followed the fluid motion, they were illumi-nated by using a 30 cm wide horizontal light sheet projected 7 mm above the bottom of the tank using two argon-ion lasers at between 4 and 8 W. Particle images were filmed using a second digital high-speed camera: either a RedLake camera at 250 fps and 480 pixel×420 pixel resolution or a NAC Hi-DCam at 500 fps at 1280 pixel×1024 pixel resolution (as in Tytell & Lauder 2004).

The flow tank's boundary layer for the floor of the working sec-tion was measured to verify that the horizontal light sheet was above the boundary layer. At the lowest flow speeds, the boundary layer was turbulent and *ca.* 7 mm thick. The boundary layer is thinner at higher flow speeds (Schlichting 1979); therefore, the light sheet was always above the boundary layer. Nevertheless, portions of the eels' bodies were in the boundary layer and ground effects could affect the flow field (Rayner & Thomas 1991).

At each swimming speed, the eel was removed and a mean background flow field was measured and subtracted from all flow fields at that speed.

(b) Data analysis

Eel outlines and midlines were digitized by using a custom MATLAB 6.1 (Mathworks, Natick, MA, USA) program. After manual identification of an eel's head and tail, the program ident-ified the outline and midline of the eel image using a cross-corre-lation based technique. Midlines were smoothed simultaneously in both space and time using a smoothing spline to achieve a mean squared error of *ca.* 0.25 square pixels (as recommended by Walker (1998)). Steady swimming kinematics and hydrodyn-amics were quantified as in Tytell (2004). Kinematic parameters, including undulation amplitude at 20 points along the body, undulation frequency, average tail-tip velocity, body wave speed and body wave length, were calculated from these midlines. Strouhal number (*St*), defined in animal studies as the ratio of average tail velocity to swimming velocity (Triantafyllou *et al.* 2000), was also estimated. The velocity and acceleration of the body were taken from the point at the tip of the snout. All variables involving a length were normalized by the eel's body length *L*.

The particle image velocimetry (PIV) algorithm was performed by using a custom MATLAB 6.1 program in two passes using a stan-dard statistical cross-correlation (Fincham & Spedding 1997) and an error-correction technique with an integer pixel estimate of the velocity between passes (as in Hart 1999). Data were smoothed and interpolated onto a regular grid using an adaptive Gaussian window algorithm with the optimal window size (2–3 mm for these data; Fincham & Spedding 1997) accounting for the uneven spacing of PIV data (Fincham & Spedding 1997).

Axial wake momentum was quantified from the flow field data. Any axial momentum was attributed to acceleration because eels have little axial flow in their wakes during steady swimming. In particular, this momentum represents differences in thrust from the amount necessary to counteract drag, and includes

components of the inertial force as well as an acceleration reaction force. The wake momentum flux ΔM, which has units of force, was estimated by integrating through a plane behind the eel in each frame:

$$\Delta M = \rho h U \int_{-w}^{w} u - U \, \mathrm{d}y, \tag{2.1}$$

where ρ is the fluid density, h is the wake height, equivalent to the fish's height (Nauen & Lauder 2002) measured at mid-body, u is the instantaneous axial fluid velocity, U is the mean flow velocity, w is half the wake width, and y is the coordinate in the lateral direction. The wake width w was 40 mm and the plane was centred on the tail tip. It was placed 8 mm downstream of the eel's tail as a compromise between two issues: first, difficulties making measurements close to the body due to shadows and reflections and second, potential errors owing to turbulence or viscous effects for measurements in the far wake (Tytell & Ellington 2003). The momentum estimate was fairly robust to the plane's location within *ca.* 1 cm. The momentum flux ΔM was smoothed over time using a running average with a window length of 0.25 tail beat periods.

When a body accelerates in a fluid, it also accelerates some vol-ume of fluid surrounding it. The mass of the fluid increases the apparent mass of the body by an amount C_f, called the added mass coefficient (Batchelor 1973; Daniel 1984). To estimate C_f, the wake momentum flux was regressed on the inertial force $\rho V a$ necessary to accelerate the eel's volume V with density ρ at the estimated rate a, as follows:

$$\Delta M = (1 + C_f)\rho V a, \tag{2.2}$$

assuming that the animal's density is approximately the same as the fluid's.

(c) Statistics

Multiple regression (Quinn & Keough 2002) was performed to relate swimming speed and acceleration to body kinematics. Five kinematic variables were included in the analysis: tail amplitude, head amplitude, average tail velocity, body wave speed and body wave length. Each swimming sequence included a period of steady swimming followed by acceleration. To separate the effects of acceleration from those of swimming speed, a 'steady swimming' value (the median) of each kinematic variable was estimated in each sequence. Then, the maximum and minimum deviation of each parameter from its steady swimming value was calculated. This allowed each swimming sequence to be its own control and removed any influence of time in the analysis. The medians and deviations were used as independent variables in the regression. Because all of the measured kinematic variables increase with increasing swimming velocity (Tytell 2004) and thus increasing force, maximum deviations were assumed to correspond to maximum accelerations, and minimum deviations to minimum acceleration.

All errors are reported as s.e.m. All statistical analyses were per-formed using SYSTAT 10.2 (Systat Software, Point Richmond, CA, USA).

3. RESULTS

Kinematic and hydrodynamic data were taken from six individuals, with length L ranging from 12 to 24 cm long, each swimming at speeds from 0.6 to 1.9 $L\,\text{s}^{-1}$ and acceler-ation a from -1.4 to $1.3\,L\,\text{s}^{-2}$. From these individuals, 68 swimming sequences consisting of 1196 tail beats in total were analysed. Of these, 894 beats occurred during steady

Table 1. Multiple regression of steady swimming speed and acceleration on tail beat amplitude, head amplitude, average velocity, body wave speed and body wave length.
(The significant kinematic correlates of swimming speed and acceleration are listed below each parameter)[a]

	coefficient	standardized coefficient	t (d.f. $= 125$)	p
steady swimming speed ($L\,s^{-1}$)				
body wave speed ($L\,s^{-1}$)	1.2 ± 0.2	1.4 ± 0.3	5.29	< 0.001
tail amplitude deviation (L)	-9 ± 3	-0.24 ± 0.04	-2.83	0.005
tail velocity deviation ($L\,s^{-1}$)	0.5 ± 2	0.25 ± 0.08	3.07	0.003
acceleration ($L\,s^{-2}$)				
tail velocity deviation ($L\,s^{-1}$)	1.9 ± 0.4	0.9 ± 0.2	4.93	< 0.001

[a] ($n = 136$, from 68 swimming sequences; L, body length; t, Student's t-statistic.)

swimming ($|a| < 0.1\,L\,s^{-2}$) and 302 during acceleration. Hydrodynamic data from 23 representative datasets with 534 tail beats were analysed, of which 457 were steady and 77 were during acceleration.

A dataset was designated 'steady' when the maximum acceleration magnitude was less than $0.1\,L\,s^{-2}$. In these sets, the velocity had a maximum standard error of *ca.* 7% and in most cases the velocity variation was less than 1%. Animals were able to maintain swimming steadily from *ca.* 0.5 to $2\,L\,s^{-1}$, corresponding to Reynolds numbers of 16 000–120 000.

(a) Steady swimming

Steady swimming data were quantified, but because similar data have been presented before (Gillis 1998; Tytell 2004), they are only briefly summarized here. Tail beat frequency, body wave length, body wave speed and average tail-tip velocity increased significantly ($p < 0.03$) with increasing swimming speed. Tail beat amplitude also increased, but not significantly ($p = 0.082$). All kinematic variables showed significant differences between individuals ($p < 0.001$ in all cases). *St* showed no significant change with swimming speed ($p = 0.202$), with a mean of 0.321 ± 0.002 across all swimming speeds, although it increased and became more variable at the slowest speeds. Undulation amplitude increased exponentially along the body.

During steady swimming, the wake consisted of lateral jets of fluid separated by one or more vortices (figure 1*a*), as described in Tytell & Lauder (2004). The angle of the jet was not significantly different from 90° to the swimming direction ($p = 0.407$), indicating a lack of significant axial flow.

(b) Acceleration

After a period of steady swimming, all eels naturally accelerated out of the filming area. Accelerations with substantial turning were identified visually and excluded. In the accelerations analysed, no eel deviated more than 40° from the flow direction and most turned less than 13°. When the entire eel was visible, the negative accelerations produced as the eels approached the front baffle or a wall were also analysed. Acceleration varied from -1.4 to $1.3\,L\,s^{-2}$.

The most obvious visual change during acceleration was an increase in body amplitude (figure 2), which was particularly noticeable at the head. Head amplitude was often close to zero, particularly at low speeds, making any small increase quite obvious. Increases in tail amplitude, although larger numerically, were less apparent visually.

Two multiple regressions were performed: one on average swimming speed with respect to kinematics, and another on acceleration versus kinematics. Both regressions were highly significant ($p < 0.001$ in both cases) and are summarized in table 1. Most coefficients were not significant, but swimming velocity is primarily predicted by body wave speed, with small contributions from tail amplitude deviation and tail velocity deviation (table 1; figure 3*a*). The variation in acceleration is only significantly related to deviation of tail velocity from the steady value (table 1; figure 3*b*).

All basic kinematic variables were correlated with each other ($r > 0.28$ in all cases), although the deviation parameters were relatively uncorrelated ($|r| < 0.09$). Correlated independent variables tend to cause underestimation of the number of significant coefficients (Quinn & Keough 2002). However, those that are significant are likely to be highly significant.

Figure 1 shows a representative flow field during steady swimming at $1.34\,L\,s^{-1}$ (figure 1*a*) and during acceleration at $0.6\,L\,s^{-2}$ (figure 1*b*). Before accelerating, the eel in figure 1*b* was swimming at $1.42\,L\,s^{-1}$. Note the reorientation of the jets (region 1) to point downstream. In the acceleration, maximum momentum flux in the wake was 4.65 mN (as a force coefficient: 0.0074), compared with the maximum force to accelerate the eel's mass alone of 1.28 mN (force coefficient: 0.0020).

As in figure 1*b*, more momentum is usually present in the wake than is accountable directly to inertial forces owing to acceleration (figure 4). Maximum and minimum wake momentum flux, equivalent to the net force on the animal, were regressed on maximum and minimum inertial force to cause the acceleration in a vacuum. This analysis produces a slope of 3.8 ± 0.6, which is significantly different from 1 ($p < 0.001$). Therefore, from equation (2.2), the added mass coefficient over the range of accelerations examined is 2.8 ± 0.6 (s.e.m.; $n = 46$, from 23 swimming sequences).

4. DISCUSSION

This study identifies the primary kinematic parameters that the American eel, *A. rostrata*, uses to control swimming speed and linear acceleration and relates this acceleration to changes in axial wake momentum. This provides the first quantitative examination, to the author's knowledge, of routine linear accelerations during fish swimming. Multiple regression indicates that the most important kinematic parameters are body wave speed and tail-tip velocity. These results suggest that *St* (Triantafyllou *et al.* 2000),
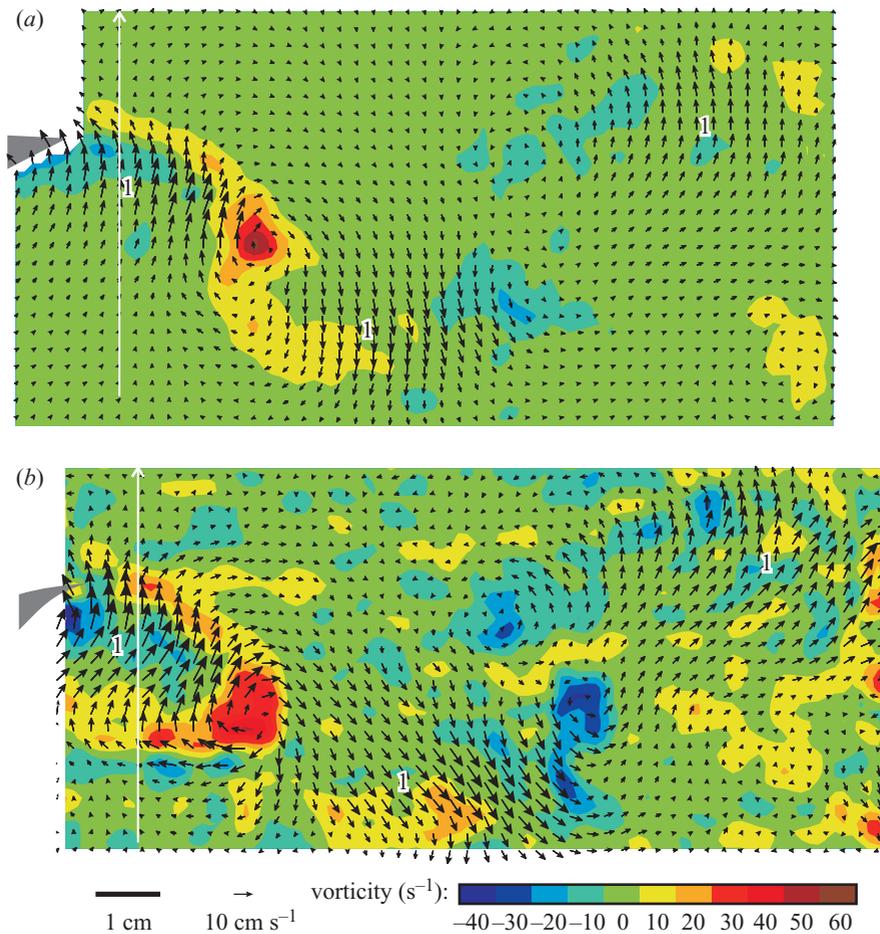
Figure 1. Representative wake flow fields. (a) Steady swimming at $1.34\,L\,s^{-1}$ by a 23 cm eel. The field is an average of 14 steady tail beats at the same phase. (b) Acceleration towards the left at $0.6\,L\,s^{-2}$, starting from steady swimming at $1.42\,L\,s^{-1}$ by a 24 cm eel. The field is an average of three fields at the same tail beat phase. In both panels, the tail tip is indicated on the left in grey, vector lengths are proportional to flow magnitude, and vorticity is given by the coloured background. For velocities less than $5\,cm\,s^{-1}$, arrowheads remain visible to indicate flow direction. Important flow regions are indicated by numbers and explained in the text. The integration plane for equation (2.1) is shown by a white line in both frames. An arrowhead indicates that the plane extends beyond the region shown.

usually written as a function of tail beat amplitude A, frequency f, and swimming speed U as $St = 2fA/U$, may be a major kinematic parameter relating to thrust output of swimming eels.

During steady swimming, St stays approximatey constant. All basic kinematic variables are correlated with swimming speed ($r > 0.38$; mean $r = 0.63$), although only body wave speed has a significant regression coefficient, possibly owing to the correlation between the kinematic variables (Quinn & Keough 2002). Nonetheless, the correlations mean that the kinematic parameters stay approximately constant fractions of swimming speed, resulting in a St that does not vary significantly with speed. During steady swimming St remains near 0.32, a value shown to be efficient for flapping propulsion (Read *et al.* 2003), and used by many animals (Triantafyllou *et al.* 2000; Taylor *et al.* 2003). Even though the swimming kinematics are correlated with speed, as steady speed drops below $1\,L\,s^{-1}$, St tends to grow and become more variable, increasing to *ca.* 0.5 at $0.5\,L\,s^{-1}$, similar to observations from some other fishes (E. Drucker, personal communication) and marine mammals (Rohr & Fish 2004). The elevation of St at low speed may not indicate decreased efficiency, because the overall metabolic cost of transport is

still low for eels swimming at $0.5\,L\,s^{-1}$ (van den Thillart *et al.* 2004). The mechanical reasons for the low cost of transport, however, remain unclear.

During acceleration, tail-tip velocity deviates from its steady value (figure 3b; $p < 0.001$), indicating a corresponding change in St. Because tail-tip velocity is proportional to fA, acceleration is correlated with a change in St. The exact change is difficult to quantify, however, because St is inversely proportional only to steady swimming speed, not the instantaneous velocity. Nonetheless, because these changes in St are correlated with acceleration, they must also be correlated with changes in net force on the body: specifically, an imbalance between thrust and drag. This correlation is plausible, because an engineering study on flapping foils found force output to be strongly related to St (Read *et al.* 2003).

However, eels cannot modulate St by changing tail-tip velocity alone. The tail velocity is a function of other kinematic variables, such as frequency and amplitude or, equivalently, body wave speed, wave length and amplitude. Because tail-tip velocity seems to increase independently of body wave speed, wave length or amplitude must also change to keep wave speed constant. Unfortunately, both
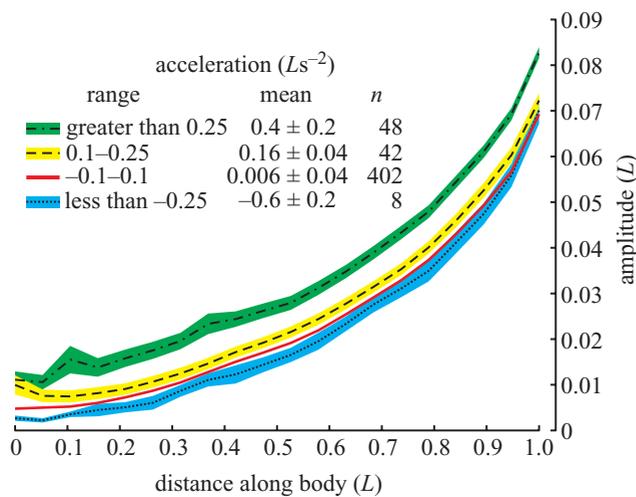
Figure 2. Undulation amplitude envelopes at each body point for different accelerations. In each case, the fish was initially swimming at about $1.5\,L\,s^{-1}$ before the acceleration. Standard error around each envelope is indicated by a coloured region. The 'steady' swimming envelope (acceleration magnitude less than $0.1\,L\,s^{-2}$) is shown by a thick red line. For each trace, acceleration ranges, mean values and number of tail beats (n) are given in the legend.

Figure 3. Multiple regression. (*a*) Swimming speed plotted against body wave speed, the best predictor of swimming speed in the multiple regression. (*b*) Acceleration plotted against tail velocity deviation, the only significant predictor of acceleration.
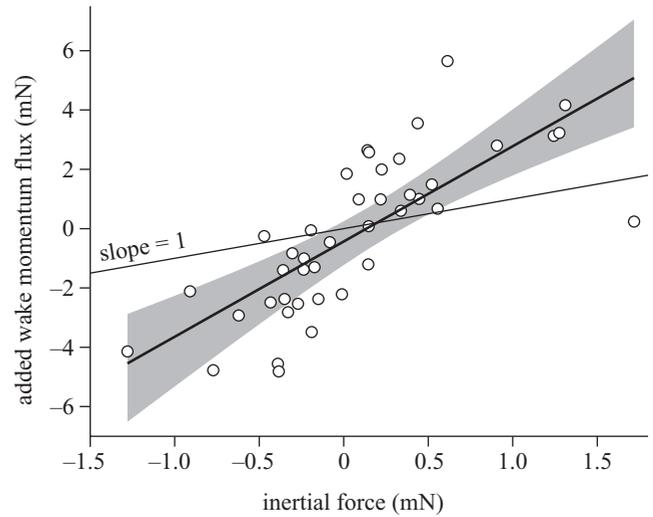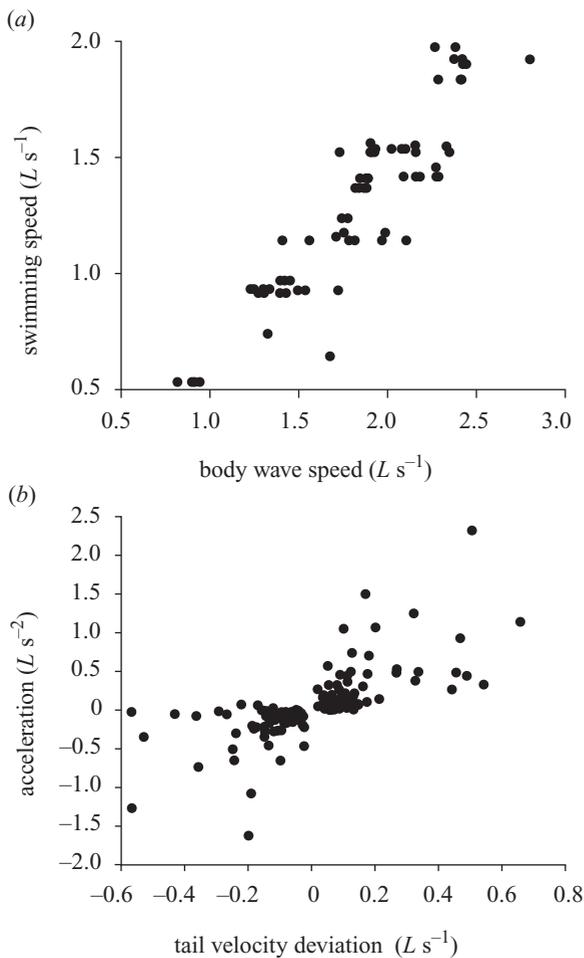
Figure 4. Added wake momentum flux plotted against inertial force due to acceleration. A linear regression line is indicated by a solid thick line with a 95% CI shown in grey ($y = (3.8 \pm 0.5)x = -0.4 \pm 0.3$; $r^2 = 0.569$; $p < 0.001$). A slope of 1 is indicated by the thin line.

of these variables have substantial noise, obscuring these trends in the data.

Nonetheless, the thrust/drag imbalance that seems to be linked to *St* deviation is apparent as axial fluid momentum in the wake. During steady swimming, when *St* remains close to 0.32, there is little or no axial momentum in the wake; all fluid momentum is directed laterally. Thus, because the net force on the fish is zero (i.e. thrust equals drag), thrust cannot be measured from the wake during steady swimming. When the eel accelerates, however, the jets rotate so that they change the axial fluid momentum (figure 1*a*), reflecting the force beyond that necessary to counter drag. This rotation causes the wake to resemble the reverse von Karman street typical of thrust production (Read *et al.* 2003) and usually observed for other fishes (see, for example, Nauen & Lauder 2002).

These qualitative changes in the wake seem quite robust, but it must be acknowledged that the quantitative hydrodynamic data in this study have limitations. Although the flow fields that have been described (figure 1) are above the boundary layer, they are only just above it, and ground effects may be substantial. However, these effects should be fairly constant within this study because all eels were of similar size. Therefore, the comparisons presented here are valid, but may be underestimates, because ground effects have been shown to lower force estimates for hovering animals (Rayner & Thomas 1991). The ground's effect for eels should be less substantial than for hovering animals (e.g. Blake 1979; Rayner & Thomas 1991), because flow is mostly parallel to the ground rather than perpendicular. Additionally, the momentum calculations may introduce some inaccuracies. Equation (2.1) assumes that flow fields are identical through the entire height of the eel, which is probably an oversimplification and might result in over- or underestimation of momentum, depending on the three-dimensional structure. Turbulent effects may also affect momentum estimates, as Tytell & Ellington (2003) found, but the method used here should be more robust to these

effects than theirs. Vertical or transverse flow fields would help to define these potential error sources.

Given these caveats, the axial momentum change seems to be significantly more than would be required to accelerate the eel's mass in a vacuum (figure 4; $p < 0.001$), indicating that linear acceleration is substantially impeded by the acceleration reaction (Batchelor 1973), with an overall added mass coefficient of 2.8 ± 0.6. In comparison, a rigid cylinder has an added mass coefficient of one accelerating perpendicular to its axis, and 0.5 parallel to its axis (Daniel 1984). Studies of oscillating cylinders have shown that the acceleration reaction can be amplified by vortex shedding owing to the oscillatory motion (Facchinetti *et al.* 2004). Extrapolating these data to eels is difficult, because the study focused on forces parallel to the oscillation direction, whereas the eel is accelerating normal to its oscillation direction. However, vortex shedding owing to oscillatory motion may have the potential to increase the effective added mass, and may be a reason why eels show such high added-mass coefficients.

Ultimately, eels appear to use different strategies for generating propulsive force during steady swimming and acceleration. By varying body wave speed proportionally to swimming speed, they can maintain steady swimming at a St known to be efficient. To accelerate, however, they vary tail-tip velocity, changing St and increasing or decreasing thrust. The decoupling of wave speed and tail velocity may help to explain how fishes control force output during unsteady swimming, a common behaviour in the wild.

REFERENCES

Batchelor, G. K. 1973 *An introduction to fluid dynamics*. Cambridge University Press.

Blake, R. W. 1979 The energetics of hovering in the mandarin fish (*Synchropus picturatus*). *J. Exp. Biol.* **82**, 25–33.

Daniel, T. L. 1984 Unsteady aspects of aquatic locomotion. *Am. Zool.* **24**, 121–134.

Domenici, P. & Blake, R. W. 1997 The kinematics and performance of fish fast-start swimming. *J. Exp. Biol.* **200**, 1165–1178.

Donley, J. M. & Dickson, K. A. 2000 Swimming kinematics of juvenile kawakawa tuna (*Euthynnus affinis*) and chub mackerel (*Scomber japonicus*). *J. Exp. Biol.* **203**, 3103–3116.

Drucker, E. G. & Lauder, G. V. 2001 Locomotor function of the dorsal fin in teleost fishes: experimental analysis of wake forces in sunfish. *J. Exp. Biol.* **204**, 2943–2958.

Facchinetti, M. L., de Langre, E. & Biolley, F. 2004 Coupling of structure and wake oscillators in vortex-induced vibrations. *J. Fluids Struct.* **19**, 123–140. (doi:10.1016/j.fluidstructs.2003.12.004)

Fincham, A. M. & Spedding, G. R. 1997 Low cost, high resolution DPIV for measurement of turbulent fluid flow. *Exp. Fluids* **23**, 449–462.

Gillis, G. B. 1998 Environmental effects on undulatory locomotion in the American eel *Anguilla rostrata*: kinematics in water and on land. *J. Exp. Biol.* **201**, 949–961.

Hart, D. P. 1999 Super-resolution PIV by recursive local-correlation. *J. Visual.* **10**, 1–10.

Jayne, B. C. & Lauder, G. V. 1995 Red muscle motor patterns during steady swimming in largemouth bass: effects of speed and correlations with axial kinematics. *J. Exp. Biol.* **198**, 1575–1587.

Müller, U. K., Smit, J., Stamhuis, E. J. & Videler, J. J. 2001 How the body contributes to the wake in undulatory fish swimming: flow fields of a swimming eel (*Anguilla anguilla*). *J. Exp. Biol.* **204**, 2751–2762.

Müller, U. K., van den Heuvel, B.-L. E., Stamhuis, E. J. & Videler, J. J. 1997 Fish foot prints: morphology and energetics of the wake behind a continuously swimming mullet (*Chelon labrosus* Risso). *J. Exp. Biol.* **200**, 2893–2906.

Nauen, J. C. & Lauder, G. V. 2002 Hydrodynamics of caudal fin locomotion by chub mackerel, *Scomber japonicus* (Scombridae). *J. Exp. Biol.* **205**, 1709–1724.

Quinn, G. P. & Keough, M. J. 2002 *Experimental design and data analysis for biologists*. Cambridge University Press.

Rayner, J. M. V. & Thomas, A. L. R. 1991 On the vortex wake of an animal flying in a confined volume. *Phil. Trans. R. Soc. Lond.* B **334**, 107–117.

Read, D. A., Hover, F. S. & Triantafyllou, M. S. 2003 Forces on oscillating foils for propulsion and maneuvering. *J. Fluids Struct.* **17**, 163–183. (doi:10.1016/S0889-9746(02)00115-9)

Rohr, J. J. & Fish, F. E. 2004 Strouhal numbers and optimization of swimming by odontocete cetaceans. *J. Exp. Biol.* **207**, 1633–1642. (doi:10.1242/jeb.00948)

Schlichting, H. 1979 *Boundary-layer theory*. New York: McGraw-Hill.

Taylor, G., Nudds, R. & Thomas, A. L. R. 2003 Flying and swimming animals cruise at a Strouhal number tuned for high power efficiency. *Nature* **425**, 707–711. (doi:10.1038/nature02000)

Triantafyllou, M. S., Triantafyllou, G. S. & Yue, D. K. P. 2000 Hydrodynamics of fishlike swimming. *A. Rev. Fluid Mech.* **32**, 33–53.

Tytell, E. D. 2004 The hydrodynamics of eel swimming. II. Effect of swimming speed. *J. Exp. Biol.* **207**, 3265–3279. (doi:10.1242/jeb.01139)

Tytell, E. D. & Ellington, C. P. 2003 How to perform measurements in a hovering animal's wake: physical modelling of the vortex wake of the hawkmoth, *Manduca sexta*. *Phil. Trans. R. Soc. Lond.* B **358**, 1559–1566. (doi:10.1098/rstb.2003.1355)

Tytell, E. D. & Lauder, G. V. 2004 The hydrodynamics of eel swimming. I. Wake structure. *J. Exp. Biol.* **207**, 1825–1841. (doi:10.1242/jeb.00968)

van den Thillart, G., van Ginneken, V., Korner, F., Heijmans, R., van der Linden, R. & Gluvers, A. 2004 Endurance swimming of European eel. *J. Fish Biol.* **65**, 312–318. (doi:10.1111/j.0022-1112.2004.00447.x)

Walker, J. A. 1998 Estimating velocities and accelerations of animal locomotion: a simulation experiment comparing numerical differentiation algorithms. *J. Exp. Biol.* **201**, 981–995.

Webb, P. W. 1991 Composition and mechanics of routine swimming of rainbow trout, *Oncorhynchus mykiss*. *Can. J. Fish. Aquat. Sci.* **48**, 583–590.